

# PTMs on H3 Variants before Chromatin Assembly Potentiate Their Final Epigenetic State

## Short Article

Alejandra Loyola,<sup>1,3,4</sup> Tiziana Bonaldi,<sup>2,3,5</sup>  
 Danièle Roche,<sup>1</sup> Axel Imhof,<sup>2</sup>  
 and Geneviève Almouzni<sup>1,\*</sup>

<sup>1</sup> CNRS UMR 218

Institut Curie

Paris 75248

France

<sup>2</sup> Histone Modifications Group and

Zentrallabor für Proteinanalytik

Adolf-Butenandt Institut

University of Munich

Schillerstrasse 44

80336 Muenchen

Germany

### Summary

Histone posttranslational modifications (PTMs) and sequence variants regulate genome function. Although accumulating evidence links particular PTM patterns with specific genomic loci, our knowledge concerning where and when these PTMs are imposed remains limited. Here, we find that lysine methylation is absent prior to histone incorporation into chromatin, except at H3K9. Nonnucleosomal H3.1 and H3.3 show distinct enrichments in H3K9me, such that H3.1 contains more K9me1 than H3.3. In addition, H3.3 presents other modifications, including K9/K14 diacetylated and K9me2. Importantly, H3K9me3 was undetectable in both nonnucleosomal variants. Notably, initial modifications on H3 variants can potentiate the action of enzymes as exemplified with Suv39HMTase to produce H3K9me3 as found in pericentric heterochromatin. Although the set of initial modifications present on H3.1 is permissive for further modifications, in H3.3 a subset cannot be K9me3. Thus, initial modifications impact final PTMs within chromatin.

### Introduction

Patterns of histone PTMs constitute the basis of the histone-code hypothesis (Jenuwein and Allis, 2001; Turner, 2002) and are thought to be important in determining specific epigenetic states. Another layer of complexity is added by the differential incorporation of histone variants (Henikoff and Ahmad, 2005; Sarma and Reinberg, 2005). Genome-wide analysis of PTMs and histone variants has led to a simple distinction between transcriptionally active and inactive regions (Mito et al., [2005] and references therein). Examples of active marks in histone H3 are H3K4me, H3K36me, and H3K9ac (according

to Turner's nomenclature [Turner, 2005]). In contrast, H3K9me and H3K27me and hypoacetylated forms are generally enriched at transcriptionally silent regions. Recent studies challenge this simple distinction with a more complex partitioning of genome marking by specific PTMs. For example, H3K9me3 is also associated with several actively transcribed genes (Vakoc et al., 2005). Although we have made enormous progress in identifying histone-modifying enzymes, how, when, and where marks are imposed in relation with a choice of a specific histone variant is poorly understood.

In mammals, there are three major classes of histone H3 variants: the replicative histones (H3.1 and H3.2), the replacement histone (H3.3), and the centromeric histone (Cenp-A) (Zweidler, 1984). H3.3 accumulates at sites of active transcription both in *Drosophila* (Ahmad and Henikoff, 2002; Schwartz and Ahmad, 2005) and mammalian cells (Chow et al., 2005; Janicki et al., 2004; Jin and Felsenfeld, 2006). Although total H3.3 derived from *Drosophila cells* (McKittrick et al., 2004), plant (Johnson et al., 2004; Waterborg, 1990), and mammals (Benson et al., 2006; Hake et al., 2006) showed enrichment in PTMs generally associated with active transcription, they did not allow a distinction between modifications present before or after chromatin assembly. The recent finding that H3 variants use distinct deposition pathways, replication independent (RI) for H3.3 and replication coupled (RC) for H3.2 and H3.1 (Henikoff and Ahmad, 2005; Kamakaka and Biggins, 2005; Nakatani et al., 2004) further emphasizes the importance of defining when PTMs are imposed and whether premodifications can impact additional marks.

To investigate how and when PTM patterns are imposed, we used epitope-tagged H3.1- and H3.3-expressing cell lines, which have proven helpful to isolate complexes competent for RC- and RI-variant deposition, respectively (Tagami et al., 2004). We generated H3.1 and H3.3 complexes from nonchromatin-bound histones, mononucleosomes, and oligonucleosomes and quantitatively analyzed PTMs of histones H3 and H4. Our study reveals that specific degrees of K9 methylation exist on nonnucleosomal histone variants. Furthermore, our data support the view that a preexisting K9 modification impacts the occurrence of H3K9me3, illustrating the ability of preexisting marks to influence further modifications.

### Results

#### Isolation of Mononucleosomal, Oligonucleosomal, and Nonnucleosomal H3.1- and H3.3-Containing Complexes

We used classical biochemical fractionation to generate cytosolic, nuclear, and chromatin extracts from epitope-tagged H3-expressing cell lines (e-H3). We then isolated e-H3.1 or e-H3.3 complexes in either nonnucleosomal or nucleosomal forms by affinity purification (Figures 1A, 2A, and 2B). In addition to selectively purifying nucleosomal or nonnucleosomal complexes that contain particular variants, this method ensures reproducibility by

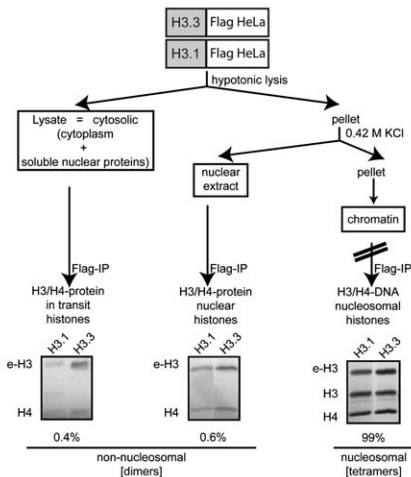
\*Correspondence: [genevieve.almouzni@curie.fr](mailto:genevieve.almouzni@curie.fr)

<sup>3</sup>These authors contributed equally to this work.

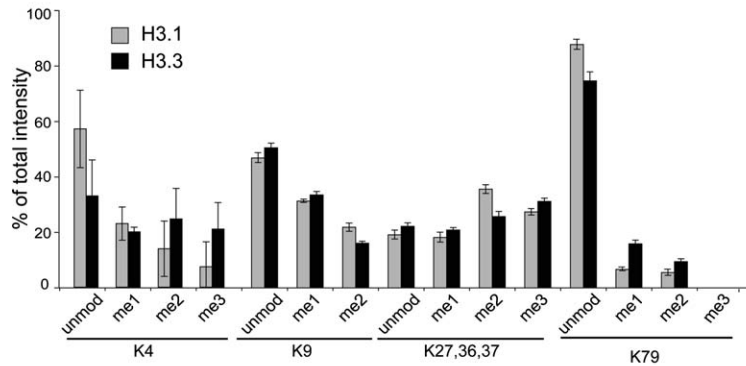
<sup>4</sup> Present address: Department of Biochemistry and Molecular Biology, M.D. Anderson Cancer Center, University of Texas, Houston, Texas 77030.

<sup>5</sup> Present address: Department of Proteomics and Signal Transduction, Max-Planck Institute of Biochemistry, D82152 Martinsried, Germany.

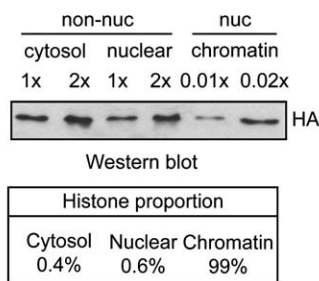
### A Purification scheme



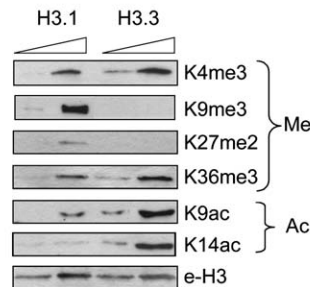
### C PTMs of nucleosomal e-H3



### B Histone proportion



### D PTMs of nucleosomal e-H3



### E Nucleosomal H4 acetylation

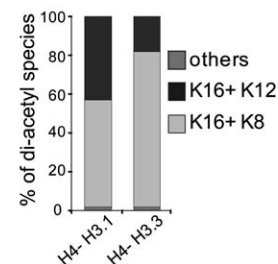


Figure 1. Analysis of e-H3 and H4 Derived from H3.1 and H3.3 Mononucleosomes

(A) Scheme for the preparation of fractions used for Flag purification. Coomassie blue-stained gels showed typical products used for MS analysis.

(B) Proportion of histones in cytosolic, nuclear, and chromatin fraction. We loaded cytosolic and nuclear extracts at the same dilution and a 100-fold dilution for chromatin.

(C) Comparison of PTMs on e-H3.1 (light bars) and e-H3.3 (dark bars). The graphs represent MALDI-MS analysis, and error bars were derived from three independent biological replicates. H3K4 peaks are generally weak and notoriously difficult to quantify, explaining the higher error bars obtained in their quantitation.

(D) We used two dilutions of H3.1 and H3.3 for western blots as indicated. HA detection provided a loading control (e-H3).

(E) Nanospray sequencing of H4 diacetylated forms. After quantification of the diacetylated species, we plotted these values as a fraction of total diacetylated H4.

using the same conditions for purification of both variants. We retrieved only e-H3 from nonnucleosomal material (dimers) and both tagged and endogenous H3 in nucleosomal fractions (tetramers) (Figure 1A). Cellular histones are distributed among chromatin, cytosol, and nuclear extract in a proportion of 99%, 0.4%, and 0.6%, respectively (Figure 1B). Expression levels of e-H3 were relatively low (both e-H3.1 and e-H3.3 variants are expressed under the regulation of the same retroviral promoter, representing about 8% of the endogenous variant) and did not affect the ratio of endogenous variants, with H3.3 representing 15% and H3.1, 53% of total histone H3 in HeLa cells (Figures S1A and S1B in the Supplemental Data available with this article online).

### PTMs on H3 and H4 Derived from H3.1 and H3.3 Mononucleosomes

We analyzed PTMs in individual histone bands in each isolated complex. Peptides were analyzed by MALDI-

TOF mass spectrometry to determine their individual mass values. In humans, H3.3 contains a serine at position 31, which is substituted to an alanine in H3.1. This substitution results in a 16 Da mass difference between H3.1 and H3.3 in the peptide (27–40) generated after digestion with arginine-specific proteases. This distinctive peptide mass allowed us to confirm the identity and homogeneity of the tagged histone samples (spectra for peptide [27–40]; H3.1= 1601.95 amu, H3.3= 1617.83 amu, Figures S2A and S3A).

Samples derived from the nucleosomal fraction showed a complex pattern of satellite peaks corresponding to different lysine methylation states with distinct profiles for H3.1 and H3.3 (Figure S2A). In contrast, cytosolic (data not shown) and nuclear complexes (Figure S3A) did not show such peaks, indicating these histones were predominantly unmodified (see below). We thus investigated whether this difference between nucleosomal and nonnucleosomal histones was unique to this peptide or whether this was a general feature

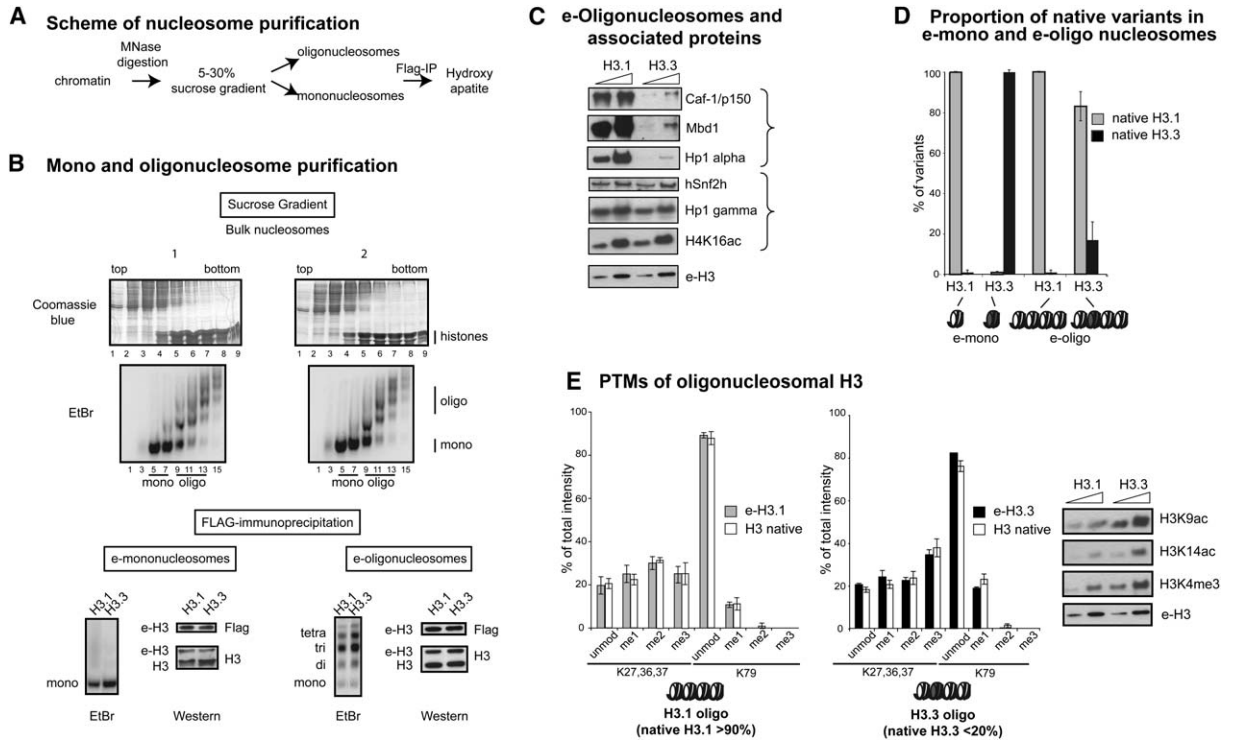


Figure 2. e-Oligonucleosomes and Associated Proteins

(A) Mono- and oligonucleosome purification scheme. (B) The top shows the sucrose gradient profiles obtained with MNase-digested samples from H3.1- (1) and H3.3- (2) expressing cells. We pooled mononucleosomes containing fractions (4–7) and oligonucleosomes (9–13) and Flag purified them (bottom). We loaded products onto 1.3% agarose (EtBr) and 15% PAGE-SDS (western blots as indicated). (C) We used two dilutions of H3.1 and H3.3 oligonucleosomes for western blots as indicated. HA detection provided a loading control (e-H3). (D) Proportion of native variants in e-mono- and e-oligonucleosomes. We analyzed and quantified the diagnostic peptide (27–40) from native H3. The graphs represent MALDI-MS analysis, and error bars were derived from two independent biological replicates. (E) Comparison of PTMs on native H3 derived from e-H3.1 (left graph) and e-H3.3 (right graph) oligonucleosomes. Light (e-H3.1) and black (e-H3.3) bars represent the analysis on the e-H3; white bars on the endogenous H3 associated with the tagged version. The graphs represent MALDI-MS analysis, and error bars were derived from two independent biological replicates. On the right, we used two dilutions of H3.1 and H3.3 oligonucleosomes for western blots as indicated. HA detection provided a loading control (e-H3).

(from now on, we will refer collectively to cytosolic and nuclear histones as nonnucleosomal histones).

MALDI-TOF analysis and western blots on e-H3.1 and e-H3.3 mononucleosomes (purification, Figures 2A and 2B) indicated these variants are enriched in distinct PTMs (Figures 1C and 1D, Figures S2A–S2C, and Table S1). As in previous analysis of total cellular histone H3 variants of *Drosophila*, *Arabidopsis*, and humans (Hake et al., 2006; Johnson et al., 2004; McKittrick et al., 2004; Waterborg, 1990), we found relative enrichment of active marks associated with H3.3. H4 isolated with either e-H3.1 or e-H3.3 mononucleosomes was mainly K20me2 (Table S1). However, we found a higher proportion of hyperacetylated H4 in mononucleosomes containing H3.3 when compared to H3.1, consistent with the general association of H3.3 with transcriptionally active regions. Importantly, a refined MS/MS analysis of diacetylated H4 N-terminal peptides revealed a bias for specific acetylation sites, with a significant increase in peptides acetylated at positions 8 and 16 in H4 derived from H3.3-containing nucleosomes. In contrast, H4 from H3.1 nucleosomes was mainly acetylated at K12 and K16 (Figure 1E and Figure S2F). A K5/K12 pat-

tern of acetylation, a hallmark of newly synthesized H4, was essentially absent in both cases.

### In Short Nucleosome Arrays, an H3.3 Nucleosome Is Flanked by H3.1 Nucleosomes that Accumulate Active Marks

We next assessed whether the distinct PTM patterns observed in mononucleosomal H3.1 and H3.3 are reflected in specific chromatin domains. Western blots of short oligonucleosomes containing H3.1 and H3.3 (Figures 2A and 2B) revealed that although some chromatin-associated proteins were associated equally with both variants (including Hp1- $\gamma$  and hSnf2h), others (such as Hp1 $\alpha$ , Mbd1, and Caf-1/p150) were enriched in H3.1 oligonucleosomes (Figure 2C). Accordingly, we found K9me3, which provides a platform for the binding of Hp1 (Maison and Almouzni, 2004), in H3.1. In contrast, H3.3 oligonucleosomes were enriched in PTMs generally associated with transcriptional activation, particularly H3K9ac, H3K14ac, and H3K4me3 (Figure 2E). We next analyzed the variant composition and associated PTMs within the short arrays. The diagnostic peptide (27–40) of the e-H3 confirmed the purity of the samples (data not

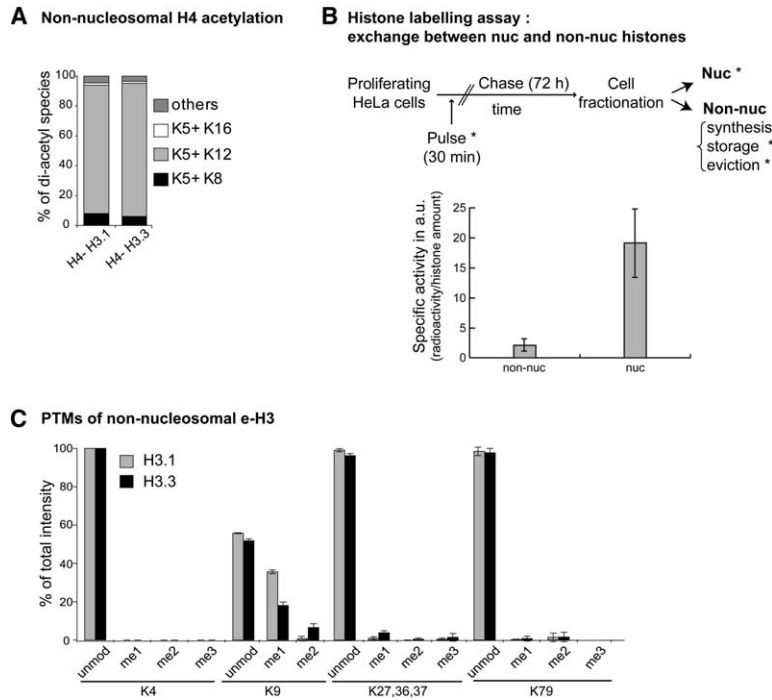


Figure 3. Analysis of e-H3 and H4 Derived from H3.1 and H3.3 Nonnucleosomes

(A) Nanospray sequencing of H4 diacetylated forms. After quantification of the diacetylated species, we plotted these values as a fraction of total diacetylated H4.

(B) Histone labeling assay. In the nonnucleosomal fraction, we expect radioactivity due to exchange or storage, but not to new synthesis. Specific activity was obtained as cpm/histone amount determined by densitometry scanning. The mean value of two independent experiments was calculated and plotted.

(C) Comparison of PTMs on e-H3.1 (light bars) and e-H3.3 (dark bars) from nonnucleosomes. The graphs represent three MALDI-MS analyses, and error bars were derived from three independent biological replicates.

shown). Analysis of endogenous H3 for this same peptide showed that H3.1 was the predominant variant in both e-H3.1 and e-H3.3 oligonucleosomes (about 80% in e-H3.3, Figure 2D). This distribution was not observed on mononucleosomes, where e-H3.3 was exclusively associated with native H3.3 and e-H3.1 to native H3.1 (Tagami et al. [2004] and Figure 2D). Because the oligonucleosomes analyzed corresponded to three to four nucleosomes on average (Figure 2B), it ensues that H3.3 is dispersed across domains, with the presence of one H3.3-containing nucleosome out of three nucleosomes. Thus, it was important to examine PTMs on native histone H3 associated with e-H3.3 to find out whether modifications normally found on H3.3 were present on H3.1 in these regions. Analysis of two peptides corresponding to amino acids 27–40 and 73–83 revealed that, regardless of the endogenous variant, the PTM pattern was similar to that of the associated e-H3 (Figure 2E). Even the native H3.1 associated with e-H3.3 showed a PTM pattern corresponding to H3.3 (Figure 2E, right graph). Our data demonstrate that active marks can be enriched on H3.1. Thus, histone PTMs are not necessarily intrinsic to specific variants and do not segregate in a simple mode, rather they are influenced by the surrounding chromatin neighborhood.

#### Both H3.1 and H3.3 Predeposition Complexes Show a K5/K12 Diacetylation Pattern on Histone H4

We next wanted to assess whether PTMs could be found prior to incorporation to DNA and contribute to final marking. We thus analyzed nonnucleosomal pools (from nuclear and cytosolic fractions). Previous studies showed that in nonnucleosomal pools H3.1 and H3.3 associate with histone chaperones, Caf-1 and Hira, respectively, in complexes competent for RC and RI variant deposition (Loyola and Almouzni, 2004; Tagami et al., 2004). The PTM pattern on H4 was particularly

revealing. In agreement with previous reports describing a unique combination of K5/K12 acetylation on newly synthesized H4 (Sobel et al., 1995), nonnucleosomal H4 was diacetylated at these positions in association with either H3 variant (Figures S3D and S3E). In both cases, MS/MS analysis showed an exclusive pattern corresponding to K5/K12 (Figure 3A and Figure S2F), which differs from the one observed on the nucleosomal H4 (Figure 1E). In principle, in addition to newly synthesized histones, evicted and stored histones could also contribute to the nonnucleosomal fraction. Indeed, histone eviction has been reported during transcription (Schwartz and Ahmad, 2005). However, pulse-chase experiments (Jackson, 1990; Thiriet and Hayes, 2005) and fluorescent recovery after photobleaching (FRAP) (Kimura et al., 2002; Phair et al., 2004) showed that H3 exchange is limited. To determine the contribution of evicted or stored histones versus newly synthesized histones in the nonnucleosomal fraction, especially for H3.3, we performed pulse-chase experiments (Figure 3B). We carried out a short (30 min) pulse with <sup>35</sup>S-Met/Cys and a long (72 hr) chase, corresponding to two cellular division times. If histone eviction occurs at a constant and high rate, we would expect comparable specific activity for both nucleosomal and nonnucleosomal H3 in a steady-state situation. We thus determined the specific activity of histone H3 in each pool (nucleosomal and nonnucleosomal), under conditions in which labeled histones had time to be incorporated and newly synthesized histones cannot be labeled. If we consider the specific activity of nucleosomal histones as 100%, stored or evicted pools represented less than 10% of the nonnucleosomal pool, even for H3.3 at a steady-state level. These values are consistent with the general low mobility of H3.3 determined by FRAP experiments both in pluripotent ES cells and lineage-committed cells (Meshorer et al., 2006). We cannot exclude that in highly

transcribed regions the local proportion of evicted histones may be higher.

Furthermore, each histone pool may have a different turnover rate, and evicted/stored pools could be rapidly degraded compared to the chromatin pool. In this case, although the eviction mechanism could be active, the corresponding histones would not be detected under our conditions. We conclude that nonnucleosomal histones represent a majority of predeposition forms in which H4 harbors a PTM pattern characteristic of newly synthesized histones and shows little distinction for the associated variant.

#### **Absence of Methylation Marks in Both Nonnucleosomal H3.1 and H3.3, Except for H3K9me**

Next, we analyzed the status of nonnucleosomal H3 for which there has been little information to date. Our data indicate that, in contrast to nucleosomal H3, no significant methylation occurred at H3K4, H3K27, H3K36, and H3K79 (Figure 3C and Figure S3B). Thus, active marks are not H3.3 “predetermined.”

Interestingly, we observed different patterns of H3K9 modifications in nonnucleosomal H3.1 and H3.3 (Figure 3C and Figure S3B). H3K9me1 was most prominent on H3.1 (36% in H3.1 compared to 17% in H3.3). In contrast, only H3.3 contained considerable amounts of H3K9ac. To distinguish between trimethylated and acetylated H3K9, we used tandem MS analysis on the (9–17) peptide and found acetylation corresponding to K14, with 20% enrichment in H3.3 and 7% in H3.1 (Table S1). High-resolution mass spectrometry also showed a significantly higher proportion of H3.3 molecules that carry an acetyl group at positions 9 and 14, a modification pattern not found in nonnucleosomal H3.1 (Table S1). Most remarkable was the absence of K9me3 in nonnucleosomal H3.1 and H3.3 (Table S1). These data imply that H3K9me3 occurs at the time of or after chromatin assembly and, if evicted, demethylation occurs immediately (Trojer and Reinberg, 2006). Given the low proportion of evicted/stored histones in our experimental conditions, H3 PTMs on nonnucleosomal complexes most likely reflect H3 status prior to incorporation into DNA.

#### **H3.1/H3.3 K9 Premodifications Potentiate the Activity of Suv39H1**

We then wondered whether the preexistence of H3K9me could potentiate the action of various H3K9 HMTases. We considered the four H3K9-HMTases identified so far: Eu-HMTase, G9a, SetDB1, and Suv39H1/H2 (Martin and Zhang, 2005). These HMTases can be divided into three groups according to their cellular distribution (Figure 4A). SetDB1 is both cytosolic and nuclear, Eu-HMTase and G9a are nuclear and chromatin associated, and Suv39H1 is mainly chromatin associated. SetDB1, Eu-HMTase, and/or G9a then could methylate nonnucleosomal histones. The Suv39 family of histone H3K9-HMTases could act downstream at targeted loci to promote a specific PTM pattern. Given the importance of the Suv39 family of HMTases in generating H3K9me3 to recruit Hp1 proteins (Maison and Almouzni, 2004), we wondered whether they preferentially act on premodified histones and may even be stimulated by specific preexisting marks. We performed methylation assays with H3 peptides carrying different K9me states with re-

combinant Suv39H1, SetDB1, and G9a enzymes. Consistent with Rea et al. (2000), our results showed that me2 peptides are not good substrate for Suv39H1 (Figure 4B). Remarkably, we found that me1 peptides scored as best substrates for Suv39H1. Tandem MS analysis showed that the final product of the reaction is K9me3 (data not shown). In contrast, K9me2 peptides are good substrates for recombinant G9a and SetDB1 (Figure 4B). This bias of modification on Suv39H1, which excludes K9me2 peptides and favors K9me1, could help to define a specific trimethylated state of the H3.1 variant by the Suv39 enzyme. Thus, although H3.1 K9 premodification is permissive for the generation of active as well as inactive chromatin marks, the K9me2 and K9ac present on H3.3 restricts its fate.

We then wondered whether H3K9me1 is the substrate for Suv39H1. MEFs derived from Suv39 double-null (dn) mice show that H3K9me3 is no longer enriched in DAPI-dense spots, which correspond to pericentromeric regions, but rather show an increase in H3K9me1 staining at these regions (Peters et al. [2003] and Figure 4C). This profile could be explained by the late action of Suv39, which would be missing at these sites. Although MEFs derived from knockout animals may harbor multiple genetic alterations, we hypothesized that Suv39 acts late in the process of setting up PTM patterns and wondered whether we could reverse the staining phenotype by reintroducing a wild-type Suv39. Strikingly, upon transfection of Suv39H dn cells with Suv39H1, we found that pericentromeric localization of Suv39H correlated with recovery of H3K9me3 enrichment, with a corresponding decrease in H3K9me1 enrichment (Figure 4C). This supports the idea that a premodified H3K9me1 can indeed be used as physiological substrate for Suv39H enzymes to produce H3K9me3. It also emphasizes a remarkable plasticity in the system, which can reverse the marking after many divisions in absence of the modifier and, thus, is likely to act rather late in setting up PTM pattern. This is clearly different from other marking systems that can only function during a specific time window, as in X inactivation (Heard, 2005) or polycomb repression (Rिंगrose and Paro, 2004).

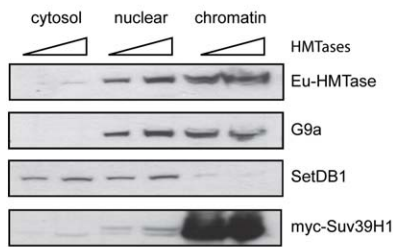
## **Discussion**

### **K9me in Nonnucleosomal H3**

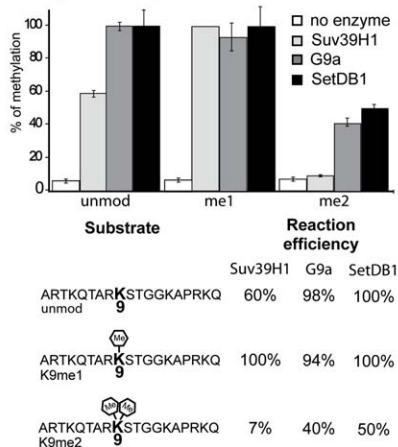
We have isolated and characterized in detail PTMs of histones H3.1 and H3.3, and associated histone H4, at different steps in the assembly line of chromatin formation. Our results show that PTMs in the mononucleosomal pool are essentially comparable to total histones, as documented by others (Benson et al., 2006; Hake et al., 2006; Johnson et al., 2004; McKittrick et al., 2004; Waterborg, 1990). Importantly, we found that oligonucleosomes containing e-H3.3 associate with H3.1, and in this context, H3.1 carries the same PTM pattern as H3.3. The data indicate that H3.1 is permissive for incorporation both into “active” and “repressive” domains. Therefore, we infer that specific PTMs, rather than the identity of the histone variant, determine the fate of a given locus.

Our analysis of nonnucleosomal H3.1 and H3.3 complexes revealed that H3K9 is the only methylated residue prior to deposition. Future studies will aim to identify the

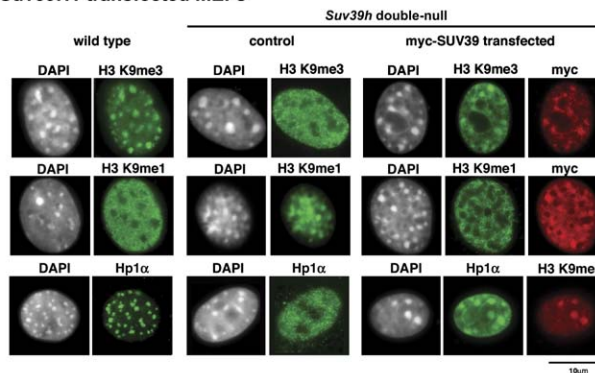
**A H3K9 HMTases in nucleosomal and non-nucleosomal fractions**



**B Peptide assay**



**C Suv39H1 transfected MEFs**



**D Stepwise model to establish and maintain PTM patterns**

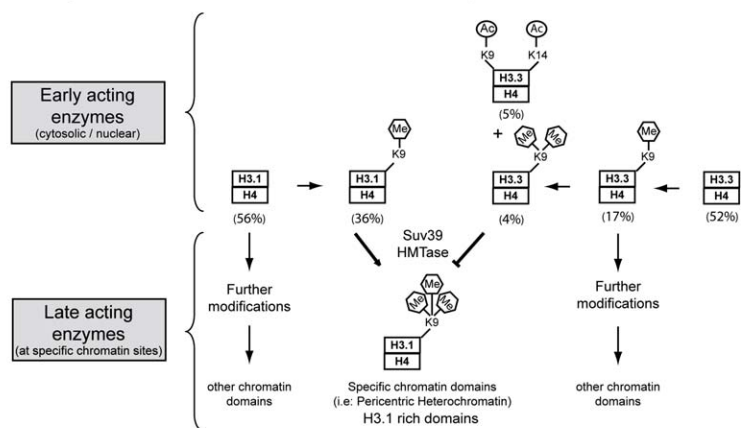


**Figure 4. Nucleosomal and Nonnucleosomal H3K9 HMTases**

(A) We detected various H3K9 HMTases by using 15 and 30 μg of cytosolic, nuclear, and chromatin extract by western blots as indicated. (B) HMTase assay with recombinant Suv39H1, G9a, and SetDB1 enzymes using unmodified, K9me, and K9me2 H3 peptides. Error bars were derived from three independent experiments. (C) We revealed by immunofluorescence, H3K9me1, H3K9me3, Hp1α and myc in wild-type and *Suv39H* dn MEFs. In addition, for dn cells, to restore wild-type staining patterns, we transfected them with myc-tagged Suv39h1 DNA. Scale bar, 10 μm. (D) Stepwise model to establish and maintain PTM patterns. The stepwise model proposes that early-acting enzymes modify nonnucleosomal H3.1 and H3.3, establishing the prenucleosomal PTM pattern. The use of different chromatin assembly pathways, RC (Caf-1 dependent) and RI (Hira-dependent), will lead to incorporation of each premodified variant. Although premodified H3.1K9me1 is permissive for K9me3 by Suv39 enzymes (late-acting enzyme) during or after DNA incorporation, the H3.3K9me2 and H3K9acK14ac fractions are more restrictive. Thus, the repertoire of permissive/restrictive initial modifications impacts the fate of a variant in specific chromatin domains.

enzymes involved in the formation of the nonnucleosomal PTM pattern. Based on subcellular distribution, it is tempting to consider SetDB1 as a prime candidate for methylation of nonnucleosomal H3, but new enzymes that remain to be discovered must also be considered. Interestingly, nonnucleosomal H3.1 and H3.3 showed a differential K9 modification pattern, which has the potential to interfere with the action of Suv39. This raises the issue of other enzymes and/or partners, which may also have a preferential choice for specific preexisting modifications to further generate PTMs. It also emphasizes the fact that H3K9me (at least me1 and me2) can be found in both active and inactive regions. This could explain how H3K9me can be found in transcribed regions (Vakoc et al., 2005). Future studies should address this issue under conditions enabling detection of dynamic changes in PTMs and also taking into account the possibility of demethylation. In any case, an important conclusion is that K9me can be found in non-nucleosomal H3 although not in a trimethylated form.

**A Stepwise Model to Define Histone PTM Patterns**

Our discovery that nonnucleosomal H3.1 and H3.3 complexes carry different levels of H3K9 modifications prior to their incorporation into chromatin, whereas other PTMs are found only in nucleosomal histones, provides the first evidence, to our knowledge, for a stepwise mechanism that culminates in the final PTM patterns found in chromatin. Figure 4D illustrates how H3K9-HMTases would function in a sequential scheme during the formation of a PTM pattern with (1) early-acting H3K9-modifying enzymes responsible for me1, me2, and ac that will give rise to the initial PTM pattern, which potentially distinguishes H3.1 from H3.3, and (2) later-acting H3K9-HMTases, responsible for me3. Mammalian Suv39 enzymes would fall into this latter category to define the typical marking found at pericentric heterochromatin. The question is then whether Suv39 enzymes are targeted at a later stage or whether they become functional later. In this respect, it is interesting to note that, in mice, analysis of heterochromatin marking in

the male pronucleus after fertilization, which is essentially established “de novo,” showed that the first methylation mark observed on K9 is K9me1, whereas K9me3 is only detected at later stages (Santos et al., 2005). Thus, in this context, an uncoupling between H3K9me1 and its further modification may occur.

The specific preference of Suv39 enzymes for H3K9me1 would favor the use of H3.1, whereas me2 and ac might prevent their action on H3.3. This could thus explain the relative enrichment in Hp1 $\alpha$  that we found in H3.1 oligonucleosomes. However, it is interesting to note that a significant fraction of nonnucleosomal H3.3 is K9me1 (17%). This form could be an intermediate to obtain K9me2 or, alternatively, could also be a substrate for Suv39 type of enzymes. In the latter case, it is tempting to speculate that this fraction represents a substrate for the Suv39-dependent heterochromatinization occurring at euchromatic genes (Schultz et al., 2002). The view of a sequential scheme to impose modification may in fact be a general one whether they are intrinsic to the enzyme or associated to a specific recognition module in a complex. Indeed, the role of Wdr5 in the Mll1 complex has recently been described as specific recognition of H3K4me2 to promote the action of the Set1 enzymes (Ruthenburg et al., 2006). Therefore, in addition to the choice of an assembly pathway, a differential premarking might provide another level of regulation in the final definition of PTM patterns.

Additional enzymes, which are locally targeted, might act after these steps, to obtain the final nucleosomal PTM pattern characteristic of specific chromatin domains. Clearly, for other modifications, including H3K4me, H3K27me, H3K36me, and H4hyperac, which are exclusively found in nucleosomes, the latter scenario is the most plausible. Setting up an active state most likely requires a mechanism coupled to transcription, and several candidate enzymes have been described both for HMTases and HATs (Peterson and Laniel, 2004; Sims et al., 2003).

In light of these findings, it will be of great importance to define the optimal substrates for all known chromatin-modifying enzymes as well as their spatial and temporal order of action. The reverse reaction should also be considered now that demethylases have been uncovered. In this respect, it is intriguing for the K9 demethylases that me3 and me2 can be removed to produce me1 (Cloos et al., 2006; Klose et al., 2006). Thus again, a sequential scheme would also work in this context.

## Experimental Procedures

### Cell Lines

H3.1 and H3.3 HeLa S3 cell lines were grown as described (Tagami et al., 2004). We transfected wild-type or *Suv39h1 Suv39h2* double-null MEFs with a myc-Suv39H1-containing construct using Lipofectamine-2000 (Invitrogen) and collected cells 48 hr posttransfection.

### Histone Labeling Assay

We used  $0.25 \times 10^8$  cells, pulsed with  $150 \mu\text{Ci}/\text{mL}$   $^{35}\text{S}$ -Met/Cys (TRAN $^{35}\text{S}$ -Label, MP Biomedicals) for 30 min followed by 72 hr chase. We measured the radioactivity in nucleosomal and nonnucleosomal fractions by western blots for HA with increasing amounts of histone e-H3. We cut bands corresponding to e-H3 and counted radioactivity. We compared equivalent amounts of nucleosomal and nonnucleosomal e-H3 (measured as HA intensity by densitometry scanning), and we set at 100% the radioactivity (cpm)

in nucleosomal histones and determined the corresponding percentage in nonnucleosomal histones.

### Complex Purification and Antibodies

See the Supplemental Data.

### Histone Processing and MALDI-Mass Spectrometry

With three sets of biological material for each analysis, we used about 5–10 pmole of histones from immunoprecipitated samples separated by SDS-PAGE. Details are in the Supplemental Data.

### Nanospray Sequencing of H4 Acetylation

To determine the position of H4ac, we performed collision-induced decay (CID) fragmentation of peptides containing amino acids (4–17) followed by the analysis of the fragment spectra in a Q-STAR mass spectrometer.

### Histone Methyltransferase Assay

We used peptides containing the first 19 amino acids of H3 either unmodified or containing one or two methyl groups at K9.

### Immunofluorescence

We performed immunofluorescence after extraction with Triton X-100 to remove soluble proteins on wild-type and *Suv39h* dn MEFs with a DMR-HC (Leica) epifluorescence microscope with  $\times 63$  objective and a camera (CoolSnap Fx, Photometrics) with a resolution of 200 nm for image acquisition.

### Supplemental Data

Supplemental Data include Supplemental Experimental Procedures, Supplemental References, three figures, and one table and can be found with this article online at <http://www.molecule.org/cgi/content/full/24/2/309/DC1/>.

### Acknowledgments

We dedicate this work to Wolfram Hörz: a great scientist, mentor, and friend. We thank H. Tagami and Y. Nakatani for Flag/HA H3.1 and H3.3 cells, and antibodies (G9a and Eu-HMTase); D. Schultz for SetDB1 baculovirus; T. Jenuwein for recombinant SUV39H1, wild-type, and *Suv39h* dn MEFs; A. Bardin, S. Barton, P. Becker, P.-A. Defossez, S. Dent, E. Heard, A. Groth, and J.-P. Quivy for comments; and T. Straub for bioinformatic support. A.L. and T.B. are supported by EMBO long-term fellowships. G.A.'s team is supported by la Ligue Nationale contre le Cancer, the Commissariat à l'Energie Atomique, European Contract RTN, Collaborative Programme between the Curie Institute and the Commissariat à l'Energie Atomique, Network of Excellence Epigenome, Cancéropôle Ile-de-France, and ACI-DRAB. A.I.'s team is supported by the Deutsche Forschungsgemeinschaft.

Received: February 7, 2006

Revised: May 24, 2006

Accepted: August 23, 2006

Published: October 19, 2006

### References

- Ahmad, K., and Henikoff, S. (2002). The histone variant H3.3 marks active chromatin by replication-independent nucleosome assembly. *Mol. Cell* 9, 1191–1200.
- Benson, L.J., Gu, Y., Yakovleva, T., Tong, K., Barrows, C., Strack, C.L., Cook, R.G., Mizzen, C.A., and Annunziato, A.T. (2006). Modifications of H3 and H4 during chromatin replication, nucleosome assembly, and histone exchange. *J. Biol. Chem.* 281, 9287–9296.
- Chow, C.M., Georgiou, A., Szutorisz, H., Maia e Silva, A., Pombo, A., Barahona, I., Dargelos, E., Canzonetta, C., and Dillon, N. (2005). Variant histone H3.3 marks promoters of transcriptionally active genes during mammalian cell division. *EMBO Rep.* 6, 354–360.
- Cloos, P.A., Christensen, J., Agger, K., Maiolica, A., Rappsilber, J., Antal, T., Hansen, K.H., and Helin, K. (2006). The putative oncogene GASC1 demethylates tri- and dimethylated lysine 9 on histone H3. *Nature* 442, 307–311.

- Hake, S.B., Garcia, B.A., Duncan, E.M., Kauer, M., Dellaire, G., Shabanowitz, J., Bazett-Jones, D.P., Allis, C.D., and Hunt, D.F. (2006). Expression patterns and post-translational modifications associated with mammalian histone H3 variants. *J. Biol. Chem.* **281**, 559–568.
- Heard, E. (2005). Delving into the diversity of facultative heterochromatin: the epigenetics of the inactive X chromosome. *Curr. Opin. Genet. Dev.* **15**, 482–489.
- Henikoff, S., and Ahmad, K. (2005). Assembly of variant histones into chromatin. *Annu. Rev. Cell Dev. Biol.* **21**, 133–153.
- Jackson, V. (1990). In vivo studies on the dynamics of histone-DNA interaction: evidence for nucleosome dissolution during replication and transcription and a low level of dissolution independent of both. *Biochemistry* **29**, 719–731.
- Janicki, S.M., Tsukamoto, T., Salghetti, S.E., Tansey, W.P., Sachidanandam, R., Prasanth, K.V., Ried, T., Shav-Tal, Y., Bertrand, E., Singer, R.H., et al. (2004). From silencing to gene expression: real-time analysis in single cells. *Cell* **116**, 683–698.
- Jenuwein, T., and Allis, C.D. (2001). Translating the histone code. *Science* **293**, 1074–1080.
- Jin, C., and Felsenfeld, G. (2006). Distribution of histone H3.3 in hematopoietic cell lineages. *Proc. Natl. Acad. Sci. USA* **103**, 574–579.
- Johnson, L., Mollah, S., Garcia, B.A., Muratore, T.L., Shabanowitz, J., Hunt, D.F., and Jacobsen, S.E. (2004). Mass spectrometry analysis of Arabidopsis histone H3 reveals distinct combinations of post-translational modifications. *Nucleic Acids Res.* **32**, 6511–6518.
- Kamakaka, R.T., and Biggins, S. (2005). Histone variants: deviants? *Genes Dev.* **19**, 295–310.
- Kimura, H., Sugaya, K., and Cook, P.R. (2002). The transcription cycle of RNA polymerase II in living cells. *J. Cell Biol.* **159**, 777–782, Published online December 9, 2002.
- Klose, R.J., Yamane, K., Bae, Y., Zhang, D., Erdjument-Bromage, H., Tempst, P., Wong, J., and Zhang, Y. (2006). The transcriptional repressor JHDM3A demethylates trimethyl histone H3 lysine 9 and lysine 36. *Nature* **442**, 312–316.
- Loyola, A., and Almouzni, G. (2004). Histone chaperones, a supporting role in the limelight. *Biochim. Biophys. Acta* **1677**, 3–11.
- Maison, C., and Almouzni, G. (2004). HP1 and the dynamics of heterochromatin maintenance. *Nat. Rev. Mol. Cell Biol.* **5**, 296–304.
- Martin, C., and Zhang, Y. (2005). The diverse functions of histone lysine methylation. *Nat. Rev. Mol. Cell Biol.* **6**, 838–849.
- McKittrick, E., Gafken, P.R., Ahmad, K., and Henikoff, S. (2004). Histone H3.3 is enriched in covalent modifications associated with active chromatin. *Proc. Natl. Acad. Sci. USA* **101**, 1525–1530, Published online January 19, 2004.
- Meshorer, E., Yellajoshula, D., George, E., Scambler, P.J., Brown, D.T., and Misteli, T. (2006). Hyperdynamic plasticity of chromatin proteins in pluripotent embryonic stem cells. *Dev. Cell* **10**, 105–116.
- Mito, Y., Henikoff, J.G., and Henikoff, S. (2005). Genome-scale profiling of histone H3.3 replacement patterns. *Nat. Genet.* **37**, 1090–1097, Published online September 11, 2005.
- Nakatani, Y., Ray-Gallet, D., Quivy, J.-P., Tagami, H., and Almouzni, G. (2004). Two distinct nucleosome assembly pathways: dependent or independent of DNA synthesis promoted by histone H3.1 and H3.3 complexes. In *Epigenetics, Symposia on Quantitative Biology*, D.S.B. Stillman, ed. (Woodbury, NY: Cold Spring Harbor Laboratory Press), pp. 273–280.
- Phair, R.D., Scaffidi, P., Elbi, C., Vecerova, J., Dey, A., Ozato, K., Brown, D.T., Hager, G., Bustin, M., and Misteli, T. (2004). Global nature of dynamic protein-chromatin interactions in vivo: three-dimensional genome scanning and dynamic interaction networks of chromatin proteins. *Mol. Cell Biol.* **24**, 6393–6402.
- Peters, A.H., Kubicek, S., Mechtler, K., O'Sullivan, R.J., Derijck, A.A., Perez-Burgos, L., Kohlmaier, A., Opravil, S., Tachibana, M., Shinkai, Y., et al. (2003). Partitioning and plasticity of repressive histone methylation states in mammalian chromatin. *Mol. Cell* **12**, 1577–1589.
- Peterson, C.L., and Laniel, M.A. (2004). Histones and histone modifications. *Curr. Biol.* **14**, R546–R551.
- Rea, S., Eisenhaber, F., O'Carroll, D., Strahl, B.D., Sun, Z.W., Schmid, M., Opravil, S., Mechtler, K., Ponting, C.P., Allis, C.D., et al. (2000). Regulation of chromatin structure by site-specific histone H3 methyltransferases. *Nature* **406**, 593–599.
- Ringrose, L., and Paro, R. (2004). Epigenetic regulation of cellular memory by the Polycomb and Trithorax group proteins. *Annu. Rev. Genet.* **38**, 413–443.
- Ruthenburg, A.J., Wang, W., Graybosch, D.M., Li, H., Allis, C.D., Patel, D.J., and Verdine, G.L. (2006). Histone H3 recognition and presentation by the WDR5 module of the MLL1 complex. *Nat. Struct. Mol. Biol.* **13**, 704–712.
- Santos, F., Peters, A.H., Otte, A.P., Reik, W., and Dean, W. (2005). Dynamic chromatin modifications characterise the first cell cycle in mouse embryos. *Dev. Biol.* **280**, 225–236.
- Sarma, K., and Reinberg, D. (2005). Histone variants meet their match. *Nat. Rev. Mol. Cell Biol.* **6**, 139–149.
- Schultz, D.C., Ayyanathan, K., Negorev, D., Maul, G.G., and Rauscher, F.J., III. (2002). SETDB1: a novel KAP-1-associated histone H3, lysine 9-specific methyltransferase that contributes to HP1-mediated silencing of euchromatic genes by KRAB zinc-finger proteins. *Genes Dev.* **16**, 919–932.
- Schwartz, B.E., and Ahmad, K. (2005). Transcriptional activation triggers deposition and removal of the histone variant H3.3. *Genes Dev.* **19**, 804–814, Published online March 17, 2005.
- Sims, R.J., III, Nishioka, K., and Reinberg, D. (2003). Histone lysine methylation: a signature for chromatin function. *Trends Genet.* **19**, 629–639.
- Sobel, R.E., Cook, R.G., Perry, C.A., Annunziato, A.T., and Allis, C.D. (1995). Conservation of deposition-related acetylation sites in newly synthesized histones H3 and H4. *Proc. Natl. Acad. Sci. USA* **92**, 1237–1241.
- Tagami, H., Ray-Gallet, D., Almouzni, G., and Nakatani, Y. (2004). Histone H3.1 and H3.3 complexes mediate nucleosome assembly pathways dependent or independent of DNA synthesis. *Cell* **116**, 51–61.
- Thiriet, C., and Hayes, J.J. (2005). Replication-independent core histone dynamics at transcriptionally active loci in vivo. *Genes Dev.* **19**, 677–682.
- Trojer, P., and Reinberg, D. (2006). Histone demethylases and their impact on epigenetic. *Cell* **125**, 213–217.
- Turner, B.M. (2002). Cellular memory and the histone code. *Cell* **111**, 285–291.
- Turner, B.M. (2005). Reading signals on the nucleosome with a new nomenclature for modified histones. *Nat. Struct. Mol. Biol.* **12**, 110–112.
- Vakoc, C.R., Mandat, S.A., Olenchock, B.A., and Blobel, G.A. (2005). Histone H3 lysine 9 methylation and HP1 $\gamma$  are associated with transcription elongation through mammalian chromatin. *Mol. Cell* **19**, 381–391.
- Waterborg, J.H. (1990). Sequence analysis of acetylation and methylation in two histone H3 variants of alfalfa. *J. Biol. Chem.* **265**, 17157–17161.
- Zweidler, A. (1984). Core histone variants of the mouse: primary structure and differential expression. In *Histone Genes, Structure, Organization and Regulation*, G.S. Gein, J.L. Stein, and W.F. Marzluff, eds. (New York: Wiley), pp. 339–371.